Effect of chromium content on structure and mechanical properties of Ti-7.5Mo-xCr alloys

D. J. LIN, J. H. CHERN LIN, C. P. JU*
Department of Materials Science and Engineering, National Cheng-Kung University, Tainan, Taiwan, ROC
E-mail: cpju@mail.ncku.edu.tw

The present work is a study of a series of Ti-7.5Mo-xCr alloys with the focus on the effect of chromium content on the structure and mechanical properties of the alloys. Experimental results show that low hardness, strength and modulus binary Ti-7.5Mo alloy is comprised primarily of fine, acicular martensitic α'' phase. When 1 wt % Cr is added, a small amount of β phase is retained. With 2 wt % or more chromium added, the entire alloy becomes equi-axed β phase with bcc crystal structure. The average β grain size decreases with Cr content. When the alloy contains about 2–4 wt % Cr, a metastable ω phase is present. In Ti-7.5Mo-2Cr alloy appears the highest ω intensity accompanied with high microhardness, bending strength and modulus. The ω-induced embrittling effect is most profound in Ti-7.5Mo-2Cr alloy that exhibits a terrace type fracture surface covered with numerous micron-sized dimples. The alloys with higher Cr contents show normal ductile type fractography with much larger deformation dimples. The present results indicate that Ti-7.5Mo-(4–6)Cr alloys seem to be potential candidates for implant application.

1. Introduction

Titanium and titanium alloys are popularly used today in many medical applications due to their light weight, excellent mechanical properties and corrosion resistance. The relatively low strength commercially pure titanium (c.p. Ti) is used as dental implant, crown and bridge, as well as denture framework [1]. With a much higher strength, Ti-6Al-4V alloy has been widely used in a variety of load-bearing orthopedic applications, such as hip prosthesis and artificial joints [2–4]. Nevertheless, studies have shown that the release of Al and V ions from the alloy might cause some long-term health problems [5, 6].

Recently a great deal of effort has been devoted to the study of more biocompatible (without Al and V) β and near-β alloys, such as Ti-Mo [7], Ti-Mo-Zr-Fe [8], Ti-Nb-Zr [9] and Ti-Mo-Hf [10] systems. Advantages of β and near-β phase alloys include their relatively low modulus and better formability [11]. Too high a modulus of implant may cause bone resorption as a result of so-called ''stress shielding'' effect [12, 13]. Weiss *et al.* [14] and Ankem *et al.* [15] have shown that low modulus β phase alloys, that reduce the stress-shielding effect [16–18], can be processed to a higher strength level with better notch properties and toughness than such $\alpha + \beta$ alloys as Ti-6Al-4V.

A binary Ti-7.5 wt % Mo alloy with α'' phase as the major phase has been developed recently in the present authors' laboratory [19]. In as-cast state, this Ti-7.5Mo alloy has a bending strength similar to that of Ti-15Mo and Ti-13Nb-13Zr with a bending modulus even lower than both alloys. The present work is a continued research based on Ti-7.5Mo system with a focus on the effect of chromium addition on the alloy structure and mechanical properties.

2. Experimental procedure

A series of Ti-7.5 wt %Mo-xCr alloys with Cr contents up to 6 wt % were prepared from raw titanium (99.5 wt % in purity), molybdenum (99.9 wt % in purity) and chromium (99.5 wt % in purity) using a commercial arc-melting, vacuum-pressure type casting system (Castmatic, Iwatani Corp., Japan). The melting chamber was first evacuated and purged with argon, and an argon pressure of 1.5 kgf/cm^2 was maintained during melting. Appropriate amounts of metals were melted in a U-shaped copper hearth with a tungsten electrode. The ingots were re-melted three times to improve chemical homogeneity. Prior to casting, the ingots were re-melted again in an open-based copper hearth under an argon pressure of 1.5 kgf/cm^2. The difference in pressure between two chambers allowed the molten alloys to instantly drop into a graphite mold at room temperature.

The cast alloys were sectioned using a Buehler Isomet low speed diamond saw (ISOMET, Buehler LTD., Lake Bluff, Illinois, USA) to obtain specimens for various purposes. Surfaces of the alloys for microstructural study were mechanically polished via a standard metallographic procedure to a final level of 0.3 μm alumina

*Author to whom all correspondence should be addressed.

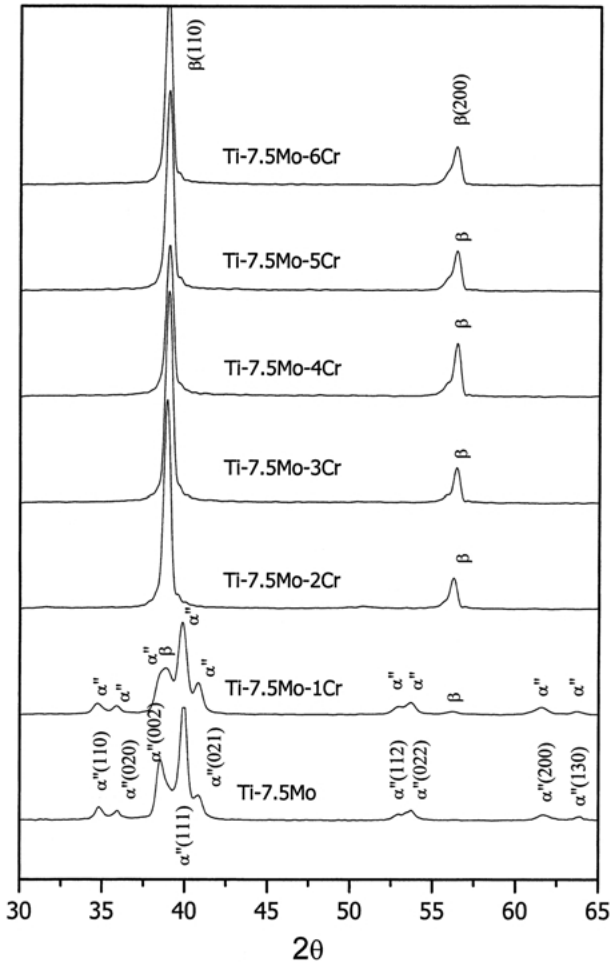

Figure 1 XRD patterns of Ti-7.5Mo and Ti-7.5Mo-xCr alloys.

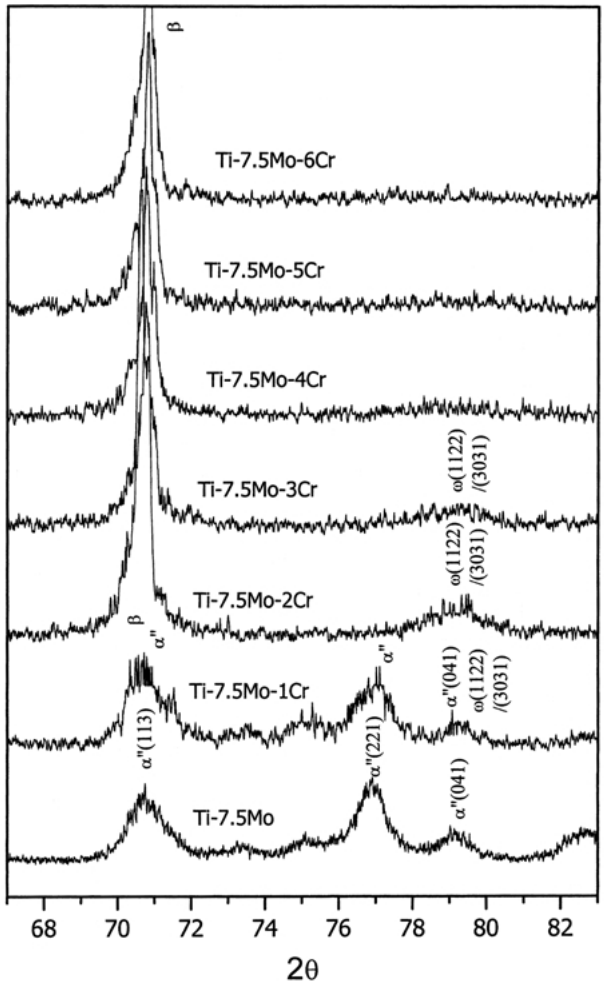

Figure 2 Lower scanning speed XRD patterns of Ti-7.5Mo and Ti-7.5Mo-xCr alloys.

powder, then etched in a Kroll's reagent comprising water, nitric acid, and hydrofluoric acid (80 : 15 : 5 in volume). Microstructure of the etched alloys was examined using an optical microscope (Leitz Labrorlux 12 Pols, Leica Co., Germany). Transmission electron microscopy (TEM) was performed using a JEOL JEM-3010 system (JEOL, Tokyo, Japan) operated at 300 KV. Thin foils for TEM were prepared using a twin jet polisher (Tenupol III, Sturers, Denmark) in an electrolyte comprising 30 ml perchloric acid (30%), 175 ml n-butyl alcohol and 300 ml methanol at $-40\,^{\circ}$C with a voltage of 12–15 V. Fractography was carried out using a field emission Philip FE-XL40 scanning electron microscope (SEM) operated at 20 kV. X-ray diffraction (XRD) for phase analysis was conducted using a Rigaku diffractometer (Rigaku D-max IIIV, Rigaku Co., Tokyo, Japan) operated at 30 kV and 20 mA. A Ni-filtered CuKα radiation was used for the study. A silicon standard was used for the calibration of diffraction angles. Scanning speeds of 0.5 and 1°/min were used.

The microhardness of polished alloys was measured using a Matsuzawa MXT70 microhardness tester at 200 gm for 15 s. Average microhardness values were obtained from at least 15 tests under each condition. Three-point bending tests were performed using a desktop mechanical tester (Shimadzu AGS-500D, Tokyo, Japan) operated at a crosshead speed of 0.5 mm/sec. Reduced size (36 × 5 × 1 mm) specimens were cut from the castings and polished using sand paper to #1000 level. The bending strengths were determined using the equation, $\sigma = 3PL/2bh^2$ [20], where σ is bending strength (MPa); P is load (Kg); L is span length (mm); b is specimen width (mm) and h is specimen thickness (mm). The modulus of elasticity in bending was calculated from the load increment and the corresponding deflection increment between the two points on a straight line as far apart as possible using the equation, $E = L^3\Delta P/4bh^3\Delta\delta$, where E is modulus of elasticity in bending (Pa); ΔP is load increment as measured from preload (N); and $\Delta\delta$ is deflection increment at midspan as measured from preload. The average bending strengths and moduli of elasticity were taken from at least six tests under each condition.

3. Results and discussion

3.1. X-ray diffraction

The XRD patterns of binary Ti-7.5Mo as well as the series of Ti-7.5Mo-xCr alloys are shown in Fig. 1. The binary Ti-7.5Mo alloy was comprised primarily of α'' phase, consistent with an earlier report of Ho *et al*. [19]. This fast cooling-induced athermal orthorhombic structure was derived from a distorted hexagonal cell in which c axis of the orthorhombic cell corresponds to c axis of the hexagonal cell with a and b corresponding to the orthogonal axis of the hexagonal cell [21]. Athermal orthorhombic martensite, that can precipitate on

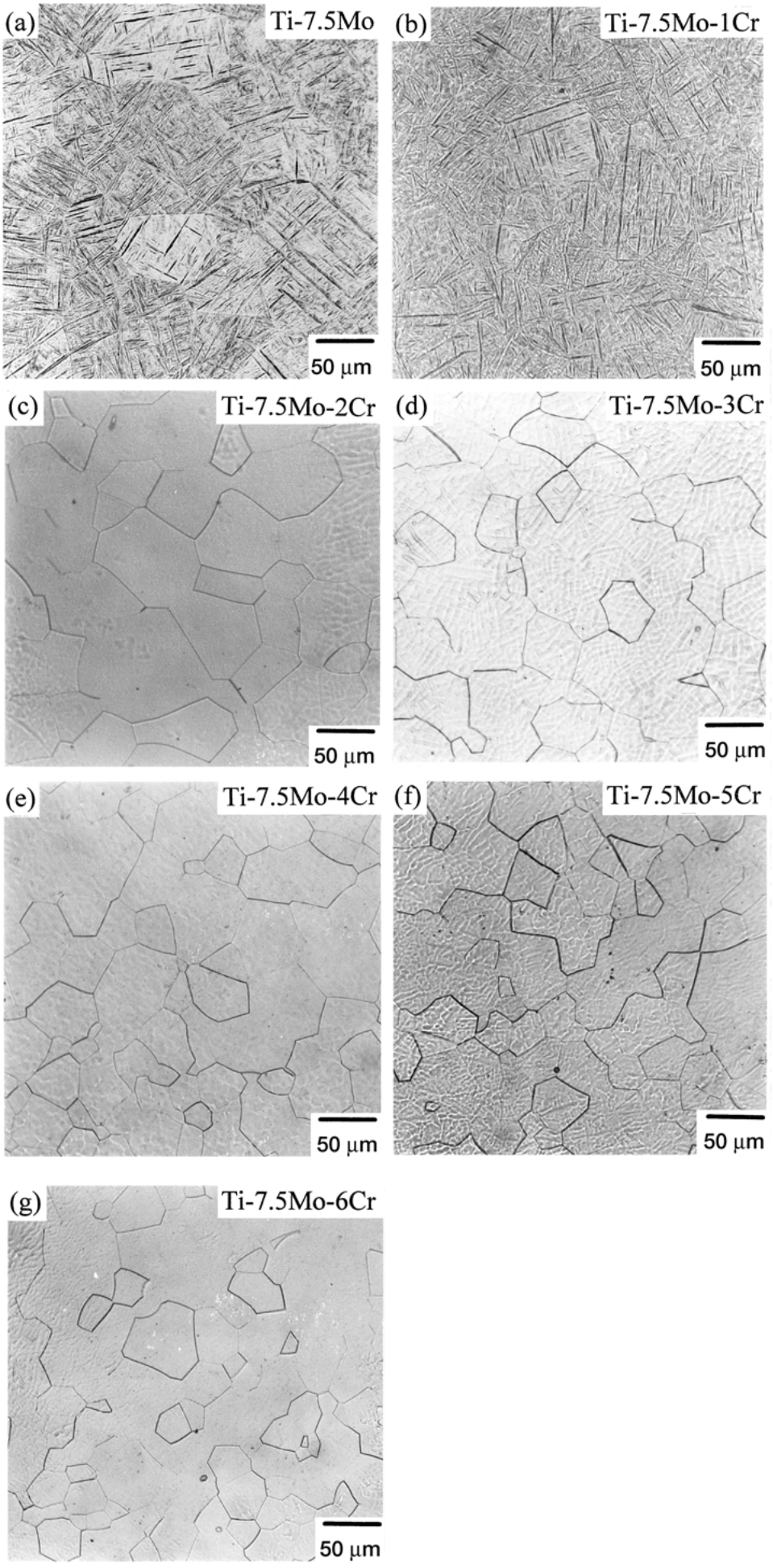

Figure 3 Light micrographs of Ti-7.5Mo and Ti-7.5Mo-xCr alloys.

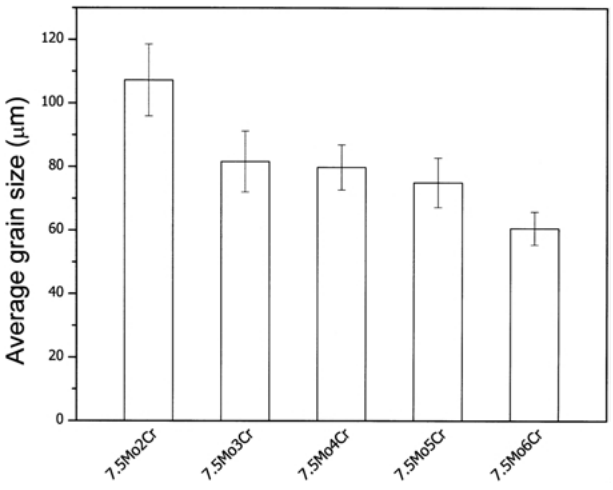

Figure 4 Average grain size of Ti-7.5Mo-xCr alloys.

quenching without the assistance of external stress, has also been reported in other Ti alloy systems [22].

As shown in Fig. 1, when 1 wt % Cr was added, a small amount of β phase started to be retained. When 2 wt % or more chromium was added, the entire alloy became β phase with a bcc crystal structure. Like Fe, Co and Ni, chromium has been recognized as an eutectoid β-stabilizing element [11]. This is true for the present Ti-Mo-Cr system. When the alloy contained about 2–4 wt % Cr, a metastable ω phase was present, as shown in the lower scanning speed (0.5°/min) XRD patterns (Fig. 2). The highest ω phase intensity appeared in the Ti-7.5Mo-2Cr alloy. The presence of this athermal ω phase, though being small in quantity, had an exceedingly important effect on the mechanical properties of the alloy, as will be discussed later.

3.2. Microstructure

Typical etched microstructure of Ti-7.5Mo and the series of Ti-7.5Mo-xCr alloys under optical microscope are shown in Fig. 3. As shown in Fig. 3(a), Ti-7.5Mo alloy exhibited a fine, acicular martensitic structure (identified as α″ phase by XRD), similar to that observed by Ho *et al*. [19]. When 1 wt % Cr was added in the alloy, β phase (identified by XRD) was observed to co-exist with α″ phase (Fig. 3(b)). When the alloy contained 2 wt % or more chromium, the entire alloy turned into an equi-axed β phase structure (Figs. 3(c)–(g)). In other words, in Ti-7.5Mo-xCr alloy system, β phase could be entirely retained upon fast cooling when the chromium content was higher than about 2 wt %. This observation is in agreement with XRD results. The average β phase grain sizes of the series of alloys, determined using a common intercept method [23], are shown in Fig. 4. As indicated in the figure, the average β grain size decreased with Cr content. The fact that Ti-7.5Mo-2Cr alloy had a much larger β grain size than those alloys with higher Cr contents indicates that the presence of ω phase did not restrict the grain growth of β phase as effectively as a higher chromium content.

Being too small to be seen by optical microscopy, the ω phase particles were quite easily resolved by TEM. Fig. 5 represents typical microstructure and selected-area diffraction (SAD) patterns of two selected alloys, Ti-7.5Mo-2Cr and Ti-7.5Mo-4Cr. Although it was difficult for XRD to detect the small amount of ω phase when the chromium content was higher than about 4 wt % (Fig. 2) due to its limited resolution, TEM clearly revealed the existence of ω phase in Ti-7.5Mo-4Cr alloy.

The overall diffraction patterns of the alloys are consistent with the report of Sass [24]. The extra reflections as marked ‘‘ + ’’ in Fig. 5(e) are a result of double diffraction [24]. It was found that the existence of ω phase was always accompanied with broadening of diffraction spots as well as diffuse streaks (diffuse scattering) [25] as a result of an incomplete (111) plane collapse from β phase. That more diffuse scattering was found in Ti-7.5Mo-4Cr than in Ti-7.5Mo-2Cr also indicates that the hcp ω structure was less ideal in the higher chromium alloy [26, 27].

Although it was not easy to accurately determine the size of ω particles in the more populated Ti-7.5Mo-2Cr alloy due to an image overlapping effect, a rough estimate indicates that the majority of these particles had sizes ranging from about 30 to 60 Å. The lattice fringes that appeared within ω particles (Fig. 5(a)) had an average spacing of approximately 4.0 Å, very close to the spacing (3.9 Å) of ω (-1010) calculated according to the diffraction pattern as shown in Fig. 5(b). This again confirms that the particles shown in the dark field image (Fig. 5(a)) are indeed ω phase particles.

The ω particles in the less populated Ti-7.5Mo-4Cr alloy showed much smaller sizes, roughly 10–20 Å, close to that found in other titanium alloys such as Ti-V [28] and Ti-Nb [29]. The consistently higher ω-to-β SAD intensity ratio of Ti-7.5Mo-2Cr alloy (Fig. 5(b) and (d)) again confirms that the lower chromium alloy comprised a larger amount of ω phase than the higher chromium alloy. This TEM observation is in agreement with the present XRD results (Fig. 2) as well as early reports of Hanada *et al*. [30] that a lower solute content titanium alloy resulted in larger athermal ω particles.

3.3. Microhardness

As indicated in Fig. 6, the α″-dominated Ti-7.5Mo alloy had the lowest microhardness (300 HV), while Ti-7.5Mo-2Cr alloy exhibited the highest microhardness level (387 HV). As described earlier, the alloy comprising 2 wt % chromium had the largest content of ω phase. This clearly indicates that ω phase is a much harder phase than α″ or β phase. When the content of ω phase decreased, the hardness decreased. When chromium content increased to 6 wt %, the hardness decreased to the same level as Ti-7.5Mo alloy.

3.4. Bending strength and modulus

Typical bending stress-deflection profiles of binary Ti-7.5Mo and the series of Ti-7.5Mo-xCr alloys are shown in Fig. 7. The average bending strengths and moduli of the alloys are given in Figs. 8 and 9, respectively. It is interesting to note that, although the average bending strengths of Ti-7.5Mo-2Cr alloy and Ti-7.5Mo-4Cr alloy were quite similar, the bending deflection of the alloy

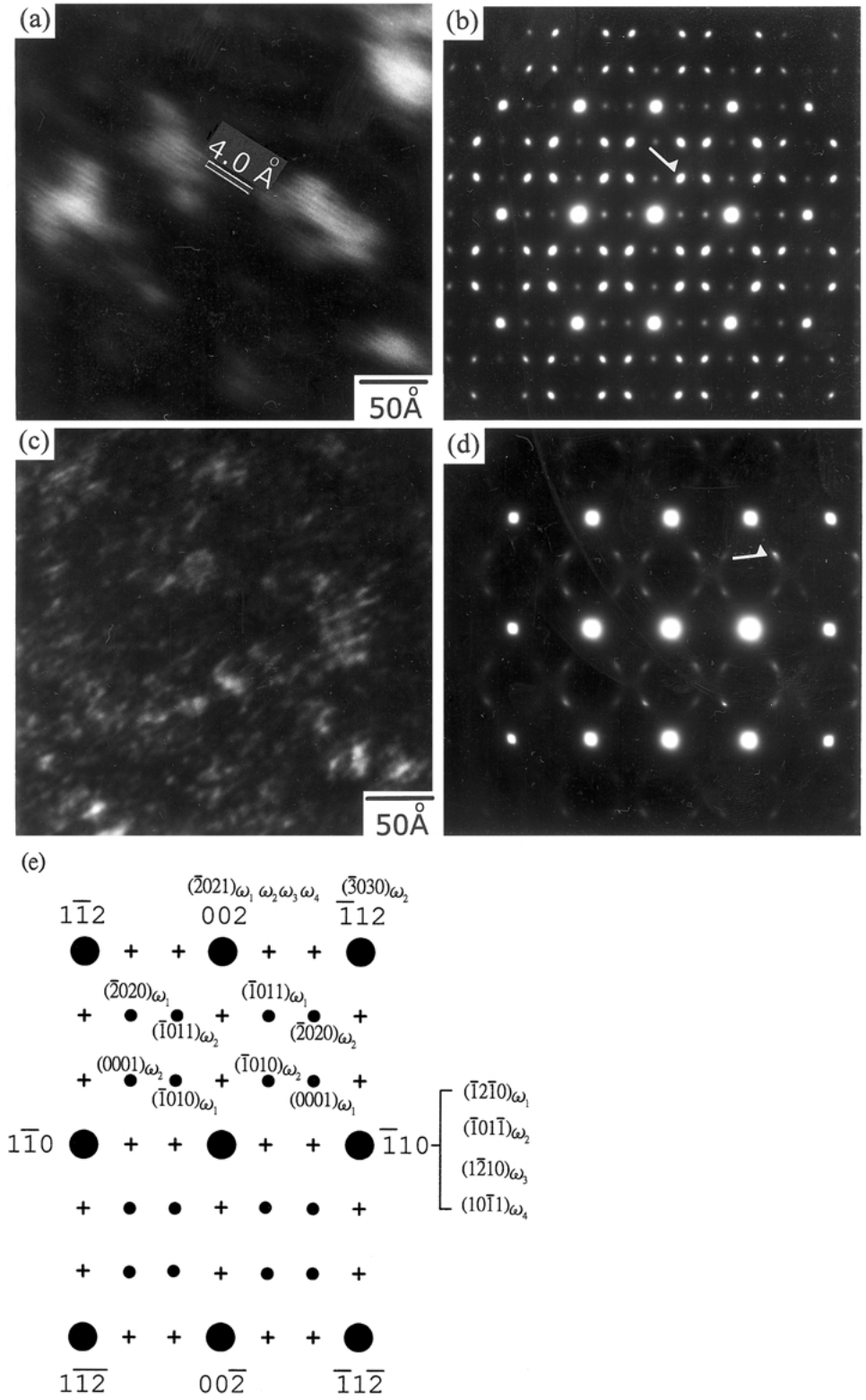

Figure 5 TEM micrographs and SAD patterns: (a) and (b) are respectively dark field image and SAD pattern of Ti-7.5Mo-2Cr alloy; (c) and (d) are respectively dark field image and SAD pattern of Ti-7.5Mo-4Cr alloy; and (e) index of diffraction pattern of bcc (110) zone.

comprising the largest amount of ω phase (Ti-7.5Mo-2Cr) was much smaller than those containing less ω. This is due to the brittle fracture that occurred to Ti-7.5Mo-2Cr but not to alloys with other compositions (Fig. 7). This ω-induced embrittlement was considered by Williams *et al*. [31] as a result of a process of nucleation, growth and coalescence of microvoids.

Despite its embrittling effect, the strengthening effect of ω phase is evident. This ω-strengthening effect is very sensitive to the chromium content of the alloy. As shown in Fig. 8, when the chromium content was only a little higher (Ti-7.5Mo-3Cr) or lower (Ti-7.5Mo-1Cr) than 2 wt %, the strengthening effect of ω phase largely diminished. It seems that this ω-strengthening effect has offset the solution strengthening effect and grain size strengthening effect that were supposed to be operative in the alloys with higher Cr contents (e.g. Ti-7.5 Mo-5Cr and Ti-7.5Mo-6Cr).

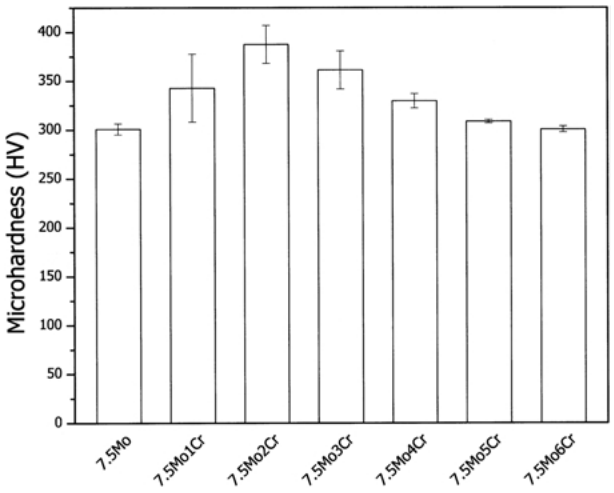

Figure 6 Microhardness of Ti-7.5Mo and Ti-7.5Mo-xCr alloys.

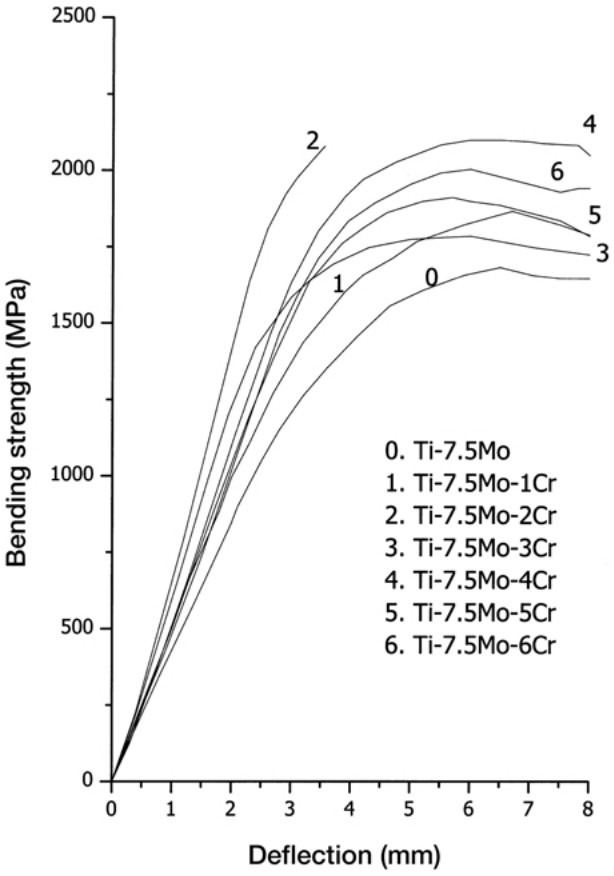

Figure 7 Typical bending stress-deflection profiles of Ti-7.5Mo and Ti-7.5Mo-xCr alloys.

As indicated in Fig. 9, the α″ phase-dominated binary Ti-7.5Mo alloy had a bending modulus of 65.4 GPa, that was lower than all those containing chromium (87–109 GPa). The low modulus nature of α″ phase has been discussed in the literature [19]. Again, the alloy comprising the largest amount of ω phase (Ti-7.5Mo-2Cr) had the highest bending modulus (109 GPa).

3.5. Fractography

The ω-induced embrittlement phenomenon was also demonstrated in the fractographic difference between those alloys with low ω content and high ω content. Fig.

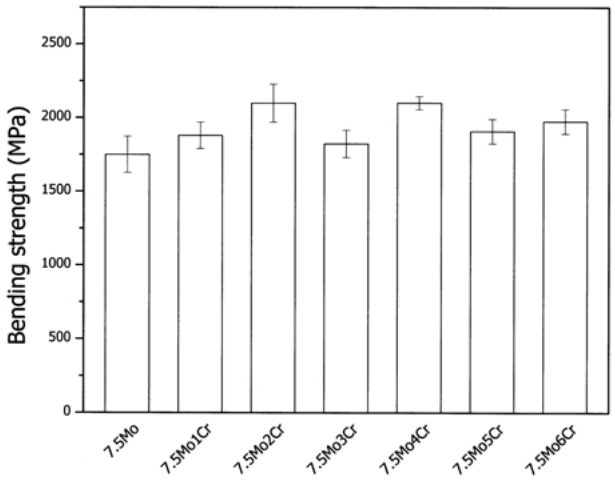

Figure 8 Bending strengths of Ti-7.5Mo and Ti-7.5Mo-xCr alloys.

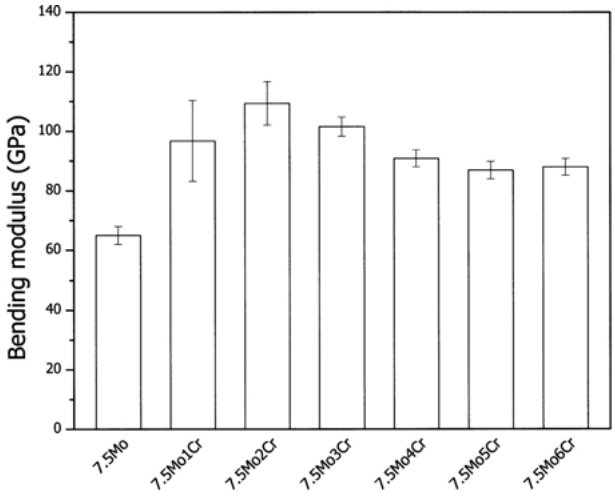

Figure 9 Bending moduli of Ti-7.5Mo and Ti-7.5Mo-xCr alloys.

10 demonstrates typical fracture surfaces of the alloy with high ω content (Ti-7.5Mo-2Cr, Fig. 10(a)) and the alloy with low ω content (Ti-7.5Mo-4Cr, Fig. 10(b)). The Ti-7.5Mo-4Cr alloy exhibited a normal ductile type fracture surface covered with deformation dimples, the majority of which had diameters 10–20 μm. On the other hand, the fracture surface of Ti-7.5Mo-2Cr alloy was featured by a terrace type morphology with numerous much smaller (1–10 μm) dimples, similar to that observed in an early study of Williams *et al.* [31] and Lin *et al.* [32]. From an engineering point of view, the chromium content of 2 wt % should be avoided, if Ti-7.5Mo-xCr alloy system is to be used due to its brittleness. For an implant material, a combination of high strength and low modulus is often desired. The present bending data indicate that the alloys with 4–6 wt % Cr seem to be potential candidates for implant application.

4. Conclusions

The low hardness, low strength and low modulus binary Ti-7.5Mo alloy was comprised primarily of fine, acicular martensitic structure α″ phase. When 1 wt % Cr was added, a small amount of β phase was retained. With 2 wt % or more chromium added, the entire alloy became

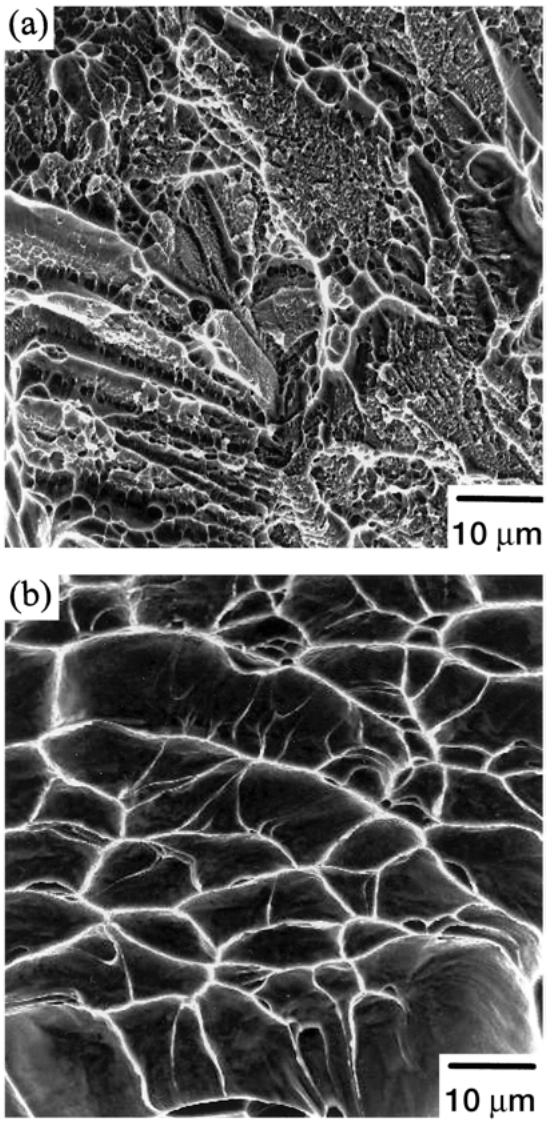

Figure 10 SEM fractographs of Ti-7.5Mo-2Cr (a) and Ti-7.5Mo-4Cr alloys (b).

equi-axed β phase with a bcc crystal structure. The average β grain size decreased with Cr content. When the alloy contained about 2–4 wt % Cr, a metastable ω phase was present. In Ti-7.5Mo-2Cr alloy appeared the highest ω intensity accompanied with high microhardness, bending strength and modulus. The ω-induced embrittling effect was most profound in Ti-7.5Mo-2Cr alloy that exhibited a terrace type fracture surface covered with numerous micronsized dimples. The alloys with higher Cr contents showed normal ductile type fractography with much larger deformation dimples. The present results indicate that Ti-7.5Mo-(4–6)Cr alloys seem to be potential candidates for implant application.

References

1. K. IDA, Y. TANI, S. TSUTSUMI, T. TOGAYA, T. NAMBU, K. SUESE, T. KAWAZOE and M. NAKAMURA, *Dent. Mater. J.* **4** (1985) 191.
2. R. VAN NOORT, *J. Mater. Sci.* **22** (1987) 3801.
3. R. L. HUCKSTEP, *Aust. N. Z. J. Surg.* **47**(3) (1977) 344.
4. M. A. IMAM and A. C. FRAKER, in: ''Medical applications of titanium and its alloys: the material and biological issues'', edited by S. A. Brown and J. E. Lemons (ASTM STP, vol. 1272, West Conshohocken, ASTM, 1996) pp. 3–16.
5. S. RAO, T. USHIDA, T. TATEISHI, Y. OKAZAKI and S. ASAO, *Biomed. Mater. Engng.* **6** (1996) 79.
6. P. R. WALKER, J. LEBLANC and M. SIKORSKA, *Biochemistry* **28** (1989) 3911.
7. L. D. ZARDIAKAS, D. W. MICHELL and J. A. DISEGI, in: ''Medical applications of titanium and its alloys: the material and biological issues'', edited by S. A. Brown and J. E. Lemons (ASTM STP, vol. 1272, West Conshohocken, ASTM, 1996) pp. 60–75.
8. K. K. WANG, L. J. GUSTAVSON and J. H. DUMBLETON, in: ''Medical applications of titanium and its alloys: the material and biological issues'', edited by S. A. Brown and J. E. Lemons (ASTM STP, vol. 1272, West Conshohocken, ASTM, 1996) pp. 76–87.
9. A. K. MISHRA, J. A. DAVIDSON, R. A. POGGIE, P. KOVACS and T. J. FITZGERALD, in: ''Medical applications of titanium and its alloys: the material and biological issues'', edited by S. A. Brown and J. E. Lemons (ASTM STP, vol. 1272, West Conshohocken, ASTM, 1996) pp. 96–113.
10. J. A. DAVIDSON, US patent No. 5954724, 1999.
11. M. J. DONACHIE, in ''Titanium: A Technical Guide'' (ASM International, Metal Park, OH, 1989) pp. 31 and 218.
12. J. B. PARK, in ''Biomaterials science and engineering'' (Plenum Press, New York, 1984) p. 143.
13. D. R. SUMNER and J. O. GALANTE, *Clin. Orthop. Relat. Res.* **274** (1992) 202.
14. I. WEISS and S. L. SEMIATIN, *Mater. Sci. Engng.* **A243** (1998) 46.
15. S. ANKEM and S. A. GREENE, *ibid.* **A263** (1999) 127.
16. K. WANG, *ibid.* **A213** (1996) 134.
17. M. NIINOMI, *ibid.* **A243** (1998) 231.
18. M. LONG and H. J. RACK, *Biomaterials* **19** (1998) 1621.
19. W. F. HO, C. P. JU and J. H. CHERN LIN, *Biomaterials* **20** (1999) 2115.
20. A. GUHA. in ''Metals Handbook'' (American Society for Metal, 9th edn, vol. 8, 1985) pp. 133–136.
21. A. R. G. BROWN, D. CLARK, J. EASTABROOK and K. S. JEPSON, *Nature* **201** (1964) 914.
22. C. BAKER, *Metal. Sci. J.* **5** (1971) 92.
23. G. F. VANDER VOORT, in ''METALLOGRAPHY Principles and Practice'' (McGraw-Hill, USA, 1984) p. 449.
24. S. L. SASS, *Acta. Metall.* **17** (1969) 813.
25. C. W. DAWSON and S. L. SASS, *Metall. Trans.* **1** (1970) 2225.
26. S. K. SIKKA, Y. K. VOHRA and R. CHIDAMBARAM, *Progr. Mater. Sci.* **27** (1982) 245.
27. E. W. COLLINGS, J. C. HO and R. I. JAFFEE, *Phys. Rev.* **B5** (1972) 4435.
28. K. K. MCCABE and S. L. SASS, *Phil. Mag.* **23** (1971) 957.
29. A. T. BALCERZAK and S. L. SASS, *Metall. Trans.* **3** (1972) 1601.
30. S. HANADA, T. YOSHIO and O. IZUMI, *J. Mater. Sci.* **21** (1986) 866.
31. J. C. WILLIAMS, B. S. HICKMAN and H. L. MARCUS, *Metall. Trans.* **2** (1971) 1913.
32. D. J. LIN, J. H. CHERN LIN and C. P. JU, *Mater. Chem. Phy.* **76** (2002) 191.

Received 17 April
and accepted 10 July 2002